

UNIVERSITY OF LATVIA
FACULTY OF PHYSICS AND MATHEMATICS



Janis Timoshenko

REVERSE MONTE CARLO MODELLING OF STRUCTURAL AND THERMAL DISORDER IN CRYSTALLINE MATERIALS

SUMMARY OF DOCTORAL THESIS

Submitted for the degree of Doctor of Physics
Subfield of solid state physics

Riga, 2015

The doctoral thesis was carried out at the Institute of Solid State Physics, University of Latvia, from year 2010 to 2014.



IEGULDĪJUMS TAVĀ NĀKOTNĒ

The work was supported by European Social Fund within the project 2009/0138/1DP/1.1.2.1.2/09/IPIA/VIAA/004 (“Support for Doctoral Studies at University of Latvia”)

The thesis consists of introduction, 8 chapters, conclusions, list of references and 5 appendices.

Type of the thesis: dissertation.

Scientific advisor: Dr. Phys. **Aleksejs Kuzmins**

Reviewers:

Dr. Chem. **Ģirts Barinovs**, docent, Faculty of Physics and Mathematics, University of Latvia, Latvia

D. Sc. **László Pusztai**, scientific advisor, Research Institute for Solid State Physics and Optics, Hungarian academy of Sciences, Hungary

Dr. Phys. **Dmitrijs Bočarovs**, researcher, Paul Scherer Institute, Laboratory for Reactor Physics and Systems Behaviour (LRS), Switzerland

The defence of the doctoral thesis will take place in an open session of the Promotion Council of Physics, Astronomy and Mechanics of the University of Latvia on the 20th of February, 2015, at 14:00 in the conference hall of the Institute of Solid State Physics, University of Latvia.

The doctoral thesis and its summary are available at the Library of the University of Latvia (19 Raina Blvd, Riga) and Latvian Academic Library (10 Rupniecības Str, Riga).

Chairperson of the Specialized Promotion Council of the scientific section of the Physics, Astronomy and Mechanics at the University of Latvia _____ Linards Skuja

Secretary of the Doctoral Committee _____ Laureta Buševica

© University of Latvia, 2015

© Janis Timoshenko, 2015

ISBN 978-9984-45-927-1

ABSTRACT

In the present thesis we develop a novel simulation-based scheme to probe the local structural and thermal disorder in crystalline materials by analyzing X-ray absorption spectra. The proposed method resembles conventional reverse Monte Carlo approach, but is more computationally efficient, as it benefits from the advantages provided by evolutionary algorithm. We believe that the proposed method improves the accuracy of currently available approaches for EXAFS analysis, especially in the case of strongly distorted local environment. The proposed approach is applied to the study of several materials such as crystalline Ge, $H_x\text{ReO}_3$, ZnO and nanocrystalline CoWO_4 and CuWO_4 .

CONTENTS

ABSTRACT	3
CONTENTS	4
GLOSSARY	5
1. INTRODUCTION	6
1.1. General introduction and motivation	6
1.2. Aim and objectives of the work	7
1.3. Scientific novelty of the work	8
1.4. Author's contribution	8
2. EXPERIMENTAL	9
3. REVERSE MONTE CARLO/EVOLUTIONARY ALGORITHM METHOD FOR EXAFS ANALYSIS	11
4. OVERVIEW OF THE MAIN RESULTS	14
4.1. Validation of proposed method	14
4.2. Hydrogen intercalation into ReO_3	16
4.3. Anisotropic dynamics of wurtzite-type zinc oxide	20
4.4. Structure of nanosized tungstates	24
5. CONCLUSIONS	27
6. MAIN THESES	30
REFERENCES	31
AUTHOR'S PUBLICATION LIST	33
Published papers	33
Papers, submitted for publication	34
Published papers that are not related to the topic of the thesis	34

GLOSSARY

DDF	Displacements distribution function
EA	Evolutionary algorithm
EXAFS	Extended X-ray absorption fine structure
FT	Fourier transform
FTIR	Fourier transform infrared spectroscopy
MC	Monte Carlo
MD	Molecular dynamics
MS	Multiple-scattering
MSD	Mean-square displacement
MSRD	Mean-square relative displacement
RDF	Radial distribution function
RMC	Reverse Monte Carlo
WT	Wavelet transform
XAS	X-ray absorption spectroscopy

1. INTRODUCTION

1.1. General introduction and motivation

The properties of materials are strongly dependent on their structure. A detailed investigation of material structure is an essential step before any technological application of the material is possible. Two the most important experimental approaches for structure studies are diffraction and X-ray absorption spectroscopy (XAS) [1]. The first one is mainly providing information on the equilibrium atomic structure, while the latter probes the instantaneous local structure of the material. Availability and evolution of synchrotron radiation sources has stimulated the development of XAS theory and methodology during the last decades, thus also the possibilities, provided by this method, are expanded significantly.

Important advantage of XAS approach in comparison to diffraction methods is that it is element-specific, thus the information on the local environment of the atoms of particular type can be obtained. Also XAS method can be applied to studies of wide range of different samples: for concentrated and for diluted systems, for crystalline and for nanostructured, amorphous, liquid samples and even for investigations of gases [2].

Extended X-ray absorption fine structure (EXAFS) is a part of X-ray absorption spectrum and contains information on the local atomic structure of the material [3]. EXAFS spectroscopy is the main experimental technique, used in this work. EXAFS experiment consists of X-ray absorption coefficient measurement as a function of the energy of incident radiation. If the energy of incident X-ray photon is sufficiently large, it excites an electron from the core state to an empty delocalized state. Such electron then can interact with electrostatic potentials of neighbour atoms, which results in the modulation of the value of absorption coefficient – an EXAFS spectrum. By analyzing such signal one can get the access to the information on average interatomic distances, relative thermal motion of atoms and static disorder. Important aspect is that EXAFS is also sensitive to many-atom distribution functions, for example, to distributions of bonding angles.

Thus an EXAFS spectrum contains an unprecedented amount of information on sample structure, but, obviously, the analysis of such complicated signal is challenging.

To address this problem, several simulation-based approaches can be used, such as classical and *ab-initio* molecular dynamics (MD), Monte Carlo (MC) and reverse Monte Carlo (RMC) methods, and different combinations of these approaches.

In all these cases a large amount of atomic configurations is generated, and one can calculate corresponding theoretical EXAFS spectrum, averaged over configurations and/or over absorbing atom sites. The obtained EXAFS spectrum then can be directly compared with the experimental data. In the MD approaches the atomic configurations are generated by the integration of classical Newton's equation of motion. The interatomic forces, required for such calculations, are given

by an empirical potential function [4], as in classical MD, or obtained in *ab-initio* calculations [5]. Empirical potential function is required also for MC simulations.

The main limitation of classical MD and MC methods is that for complicated systems with low symmetry the construction of empirical potential functions is a challenging task. *Ab-initio* MD approaches, in turn, currently are limited to very simple systems due to extreme demand for computational resources. To avoid this problem one can use RMC-type methods. In this case the generation of atomic configurations is not determined by any physical considerations, but is a random process. For each atomic configuration one calculates corresponding theoretical EXAFS spectrum that is then compared to experimentally obtained data. Accordingly to how close are the theoretical and experimental EXAFS spectra, the proposed atomic configuration is either accepted or discarded. By choosing appropriate parameters of calculations, one can ensure that after given (and usually large) number of steps the simulated atomic configuration will represent the atomic structure of the sample [6]. This method is general and can be applied to a wide range of problems. Unfortunately, it is also computationally inefficient. Thus the further development of simulation-based approaches for the EXAFS analysis is necessary.

1.2. Aim and objectives of the work

The research, presented in the thesis, consists of both experimental (EXAFS measurements at synchrotron radiation sources) and theoretical (software development and computer simulations) parts.

The main goal of the thesis is to develop novel simulation-based approach (RMC/EA-EXAFS), based on the reverse Monte Carlo method and evolutionary algorithm (EA), for the analysis of EXAFS data from crystalline and nanocrystalline materials. The novel approach inherits from the RMC method its general applicability, but is more computationally efficient. The objectives of the present work are:

- to perform temperature-dependent EXAFS studies of crystalline wurtzite type ZnO and crystalline and nanocrystalline tungstates CoWO_4 and CuWO_4 at synchrotron radiation sources;
- to demonstrate the potentiality of the method for the analysis of experimental EXAFS spectra from crystalline materials, starting with the case of monoatomic crystalline germanium, and then applying it to more complex many-atom systems such as perovskite-type ReO_3 , wurtzite-type ZnO and two wolframite-type tungstates as CoWO_4 and CuWO_4 ;
- to demonstrate the potentiality of the method for the analysis of experimental EXAFS spectra from nanocrystalline tungstates CoWO_4 and CuWO_4 ;
- to demonstrate the ability of the EXAFS technique in general to provide information on many-atom distribution functions, correlation effects and anisotropy of thermal disorder.

1.3. Scientific novelty of the work

Within this thesis a novel method for EXAFS analysis, based on the use of evolutionary algorithm, has been proposed and realized by author in the original software. The new method allowed us for the first time (i) to follow *in-situ* the development of the local structure of crystalline rhenium oxide upon intercalation of hydrogen ions and to discriminate two different effects in this process (one, related to electronic effects, and the other, related to lattice deformations); (ii) to reveal that in wurtzite-type ZnO the interactions of atoms, which lie in the same crystallographic *ab*-plane, differ significantly from the interactions of atoms, which are located at similar distances, but in different *ab*-planes, that results in the changes of the equilibrium position of oxygen atom along *c*-axis upon temperature increase; (iii) to obtain structure model for crystalline and nanocrystalline tungstates (CoWO_4 , CuWO_4), analysing simultaneously the EXAFS data at two absorption edges (Co/Cu K-edge and W L_3 -edge).

1.4. Author's contribution

The research, presented in the thesis, has been mostly carried out at the Institute of Solid State Physics, University of Latvia. The author also has taken part in 10 experiments using synchrotron radiation that have been carried out at the international synchrotron facilities as HASYLAB/DESY (Hamburg, Germany), ELETTRA (Trieste, Italy) and SOLEIL (Paris, France). In particular, the author participated in temperature-dependent EXAFS measurements of ZnO, CuWO_4 and CoWO_4 , which are directly relevant to the present work. The experimental EXAFS data on Ge and H_xReO_3 have been taken from [7] and [8], respectively.

Besides, the author participated in temperature-dependent EXAFS measurements of ZnWO_4 , MnWO_4 , SnWO_4 , NiO, Cu_3N , ScF_3 , Y_2O_3 and Fe-Cr alloys and pressure-dependent EXAFS measurements of SnWO_4 . The results of these studies are not included in the thesis, but allowed us to elaborate a novel simulation-based approach for the EXAFS data treatment.

The new approach for EXAFS analysis, based on the use of evolutionary algorithm, was proposed and developed by the author, and was implemented in the original software, written by author in C++ language. Simulations have been carried out by the author at the Latvian SuperCluster facility [9], and consequent post-processing of the obtained results has been carried out by a set of original programs, written by the author in *Wolfram Mathematica* environment. The author has participated in 7 international summer schools during 2007-2014. The results of the research have been presented at 10 international conferences. Main results have been published in 15 SCI papers, and the author is the main contributor for 9 of them.

2. EXPERIMENTAL

X-ray absorption coefficient $\mu(\hbar\omega)$ is not a smooth function of incident radiation energy $\hbar\omega$. Sharp variations, so called absorption edges, located at some specific energies, can be observed, when $\hbar\omega$ is getting large enough to make another deep core level (K, L₁, L₂, L₃, ...) to participate in the absorption processes.

Term EXAFS, Extended X-ray Absorption Fine Structure, is referred to small oscillations of μ as a function of $\hbar\omega$, located starting from about 30...40 eV above the reference energy E_0 , associated with given absorption edge, and up to about 1000 eV beyond the edge. It is common to express EXAFS spectrum $\chi(k)$ in terms of wavenumber $k = \sqrt{2m_e(\hbar\omega - E_0)/\hbar^2}$, (m_e is the electron mass, and \hbar is the Plank's constant).

In synchrotron sources X-rays are produced by bending the trajectories of fast, charged particles by strong magnetic field. Such sources have high brilliance, provide possibility to scan continuously the energy of the photons, used for experiment, and, importantly, provide radiation with sufficiently high energy to excite electrons from the atomic core levels, which is often higher than 10 keV. Thus such sources are suitable for EXAFS experiments. Within this study EXAFS measurements for ZnO (Zn K-edge, $E_0 = 9.7$ keV) and for microcrystalline and nanocrystalline tungstates CuWO₄ and CoWO₄ (Co K-edge, $E_0 = 7.7$ keV, Cu K-edge, $E_0 = 9.0$ keV, W L₃-edge, $E_0 = 10.2$ keV) have been carried out at HASYLAB/DESY synchrotron radiation facility in Hamburg.

In the conventional XAS experiment absorption spectrum is measured point by point, and the change of the energy of photons, diffracted in the sample direction, is ensured by step-by-step rotation of monochromator crystal(s). The intensity of the incident beam and the intensity of the beam that has passed through the sample are measured using ionization chambers – reservoirs, filled with inert gases and high-voltage electric field applied. The intensity of X-rays is proportional to the current, produced by drift of ionized gas atoms in the applied electric field. Various sample environments can be easily installed around the sample – e.g., nitrogen or helium cryostats, furnaces, equipment for different *in-situ* experiments.

For the XAS measurements in transmission mode the thickness and concentration of the sample should be carefully adjusted, in order to ensure appropriate signal-to-noise ratio. The sample preparation technique that ensures probably the best homogeneity of the sample for measurements in transmission mode, is the deposition on nitrocellulose Millipore filter: the powder is ground and suspended in the water or other appropriate liquid, and then is filtered through the Millipore filter using water pump, and then is fixed using Scotch or Kapton tape. This method is used for preparation of the most of the samples, analyzed in this work.¹

¹ More details regarding sample preparation and EXAFS measurements, presented within this thesis, can be found in our papers: J. Timoshenko, A. Anspoks, A. Kalinko, A. Kuzmin, TEMPERATURE DEPENDENCE OF THE LOCAL STRUCTURE AND LATTICE DYNAMICS OF WURTZITE-TYPE ZnO, *Acta Mater.* 79 (2014) 194-202, and J. Timoshenko, A. Anspoks, A. Kalinko, A. Kuzmin, ANALYSIS OF EXAFS DATA FROM COPPER TUNGSTATE BY REVERSE MONTE CARLO METHOD, *Physica Scripta* 89 (2014) 044006 (6 pages).

3. REVERSE MONTE CARLO/EVOLUTIONARY ALGORITHM METHOD FOR EXAFS ANALYSIS

Simulations based approaches allow one to obtain a 3D model of material atomic structure from its EXAFS. The 3D model is defined as a set of atomic coordinates in a sufficiently large piece of investigated material. For such model the corresponding theoretical EXAFS spectrum can be calculated using existing *ab-initio* codes [10, 11] and then compared with the experimental data. If the constructed model gives a good agreement between theoretically calculated and experimental EXAFS spectra, then one may expect that the coordinates of atoms in the model represent the atomic configuration of the real material.

Monte Carlo (MC) technique incorporates a broad class of methods that can be used to solve different types of problems. The common idea of all Monte Carlo methods is to use random rather than deterministic process [12].

Reverse Monte Carlo (RMC) method was proposed by McGreevy and Pusztai in [6, 13]. The aim of this approach was to minimize the difference between the experimental and numerically simulated diffraction and/or EXAFS data by consequent random modifications of the structure model.

Nowadays, RMC method is a well-established approach for structure investigations. Currently, however, most of the existing RMC implementations are focused on the analysis of diffraction data [14, 15] and/or on studies of disordered materials [16, 17]. The possibility to apply RMC analysis to the treatment of EXAFS data from crystalline systems taking into account all so called multiple-scattering (MS) effects, is, in turn, weakly explored due to the significant computational complexity of such task. If MS contributions are included in the analysis, usually they are treated in approximate way [18].

The goal of the presented thesis is to contribute to the advancement of this field and to provide a versatile and computationally efficient tool for RMC-EXAFS analysis of the local structure of crystalline materials.

Within this thesis a novel RMC-type method for the analysis of EXAFS data has been developed and implemented by the author in EvAX (Evolutionary Algorithm for XAS data analysis) program, written in C++ language.

Four main building blocks of our approach can be identified:

***Ab-initio* EXAFS calculations**

Excellent codes for the *ab-initio* simulations of EXAFS data are available nowadays. In our case we use the FEFF8 code by Ankudinov, Ravel, Rehr et al. [10] for this purpose: it is implemented as inner routine in EvAX program. As it is the most time-consuming part of simulations, it is necessary, however, to reduce the required number of FEFF calculations as much as possible. Therefore, first of all, in the present study we carefully examine the importance of all scattering paths and employ high-dimensional clustering algorithms

to agglomerate similar paths. Secondly, the calculations of EXAFS spectra are parallelized, to employ the potentiality of multiprocessor systems.

Signal processing

The noise should be removed from the experimental EXAFS data. Additionally, the conventional Fourier transform (FT) can be used to separate contributions from different coordination shells. However, in this study we demonstrate that the use of novel wavelet transform (WT) is preferable, since it gives the representation of the analyzed signal in real and frequency spaces simultaneously and provides more information, allowing one to better discriminate different contributions to the total EXAFS spectrum [19].

Optimization algorithms

Structure model that gives the best agreement between calculated and experimentally measured EXAFS data can be obtained by performing a search for global minimum in high-dimensional space. The reverse Monte Carlo method, based on Metropolis algorithm [12, 13], is a widely acknowledged tool for this purpose. In this study we employ for the first time for simulation-based EXAFS analysis a much more efficient approach, based on evolutionary algorithm (EA). In the EA approach several structural models are simulated instead of just one as in conventional RMC. Exchange of information between different models allows one to explore configurational space more efficiently [20].

Postprocessing of obtained results

The information on interatomic distances, bonding angles, amplitudes and correlations of atomic motion, etc., should be extracted from the obtained set of atomic coordinates; since we are dealing with relatively small structure models (supercells), the statistics is rather poor and robust statistics methods should be employed at this stage.

The basic elements of the EvAX algorithm are emphasized in Fig. 3.1. An advanced postprocessing of obtained results is realized as a separate set of interactive tools, created in *Wolfram Mathematica* environment.

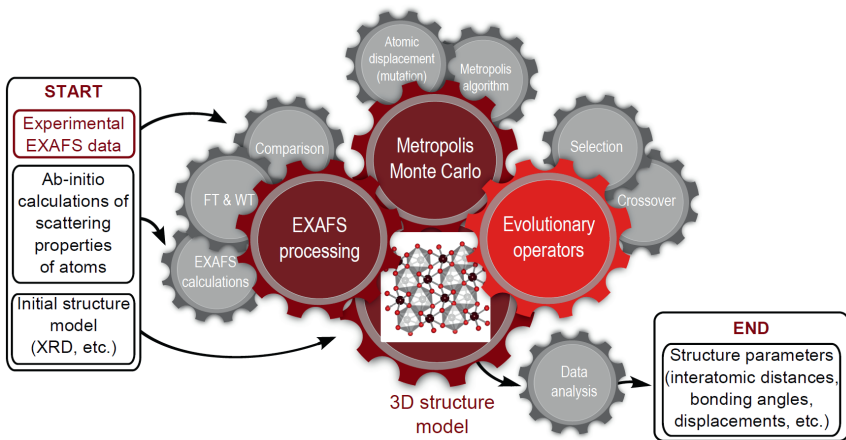


Fig. 3.1 Schematic representation of the developed EvAX algorithm

Calculation starts with some initial configuration, for instance, with equilibrium configuration known from diffraction experiments. At each iteration a new configuration is generated by randomly displacing all atoms. Configuration-averaged EXAFS spectrum is obtained in *ab-initio* calculations, and is then compared with experimental EXAFS data using Fourier or wavelet transforms. According to Metropolis algorithm, considered atomic configuration is either accepted or discarded. If EA is applied, this process is carried out for multiple configurations, and a new set of configurations is created at each iteration from the old one, using evolutionary operators: selection and crossover. The process is repeated till there is no improvement of the agreement between experimental and simulated EXAFS data. The final 3D structure model thus is consistent with experimental data and can be used to estimate the values of structure parameters of interest.

4. OVERVIEW OF THE MAIN RESULTS

4.1. Validation of proposed method²

Before applying the proposed method to experimental data, we have validated it using model EXAFS spectra, obtained from molecular dynamics (MD) simulations [21]: sets of atomic configurations, generated by MD procedure, were used to calculate configuration-averaged EXAFS spectra (MD-EXAFS) that later were used instead of experimental EXAFS data in RMC/EA calculations. In this case the true values of structural parameters, corresponding to EXAFS spectrum, were known and could be used to demonstrate the accuracy of presented approach.

Two model spectra were considered: Ge K-edge EXAFS spectrum for crystalline germanium³ and Re L₃-edge EXAFS spectrum for perovskite-type rhenium trioxide ReO₃ [21]. In both cases it was demonstrated that RMC/EA method is able to reconstruct reliably the local structure of material. Further in this section we will focus on the case of Re L₃-edge MD- EXAFS data⁴.

RMC/EA calculations for Re L₃-edge MD-EXAFS have been performed by the EvAX code, employing evolutionary algorithm with different number of simultaneously used structure models (atomic configurations).

The conventional RMC calculations (calculations with only one structure model) were unsuccessful in this case (Fig. 4.1(a)): with only one atomic configuration the given number of iterations was too small, and the system got trapped in some local minimum, thus providing the largest final residual.

² The material, presented in this section, has been published as J. Timoshenko, A. Kuzmins, J. Purans, EXAFS STUDY OF HYDROGEN INTERCALATION INTO ReO₃ USING THE EVOLUTIONARY ALGORITHM; *J. Phys.: Condens. Matter* 26 (2014) 055401 (15 pages).

³ See our paper J. Timoshenko, A. Kuzmin, J. Purans, MOLECULAR DYNAMICS SIMULATIONS OF EXAFS IN GERMANIUM, *Cent. Eur. J. Phys.* 9 (2011) 710-715 for the details of MD simulations.

⁴ Results, obtained for Ge K-edge EXAFS data, were published as J. Timoshenko, A. Kuzmin, J. Purans, REVERSE MONTE CARLO MODELLING OF THERMAL DISORDER IN CRYSTALLINE MATERIALS FROM EXAFS SPECTRA, *Comp. Phys. Commun.* 183 (2012) 1237-1245.

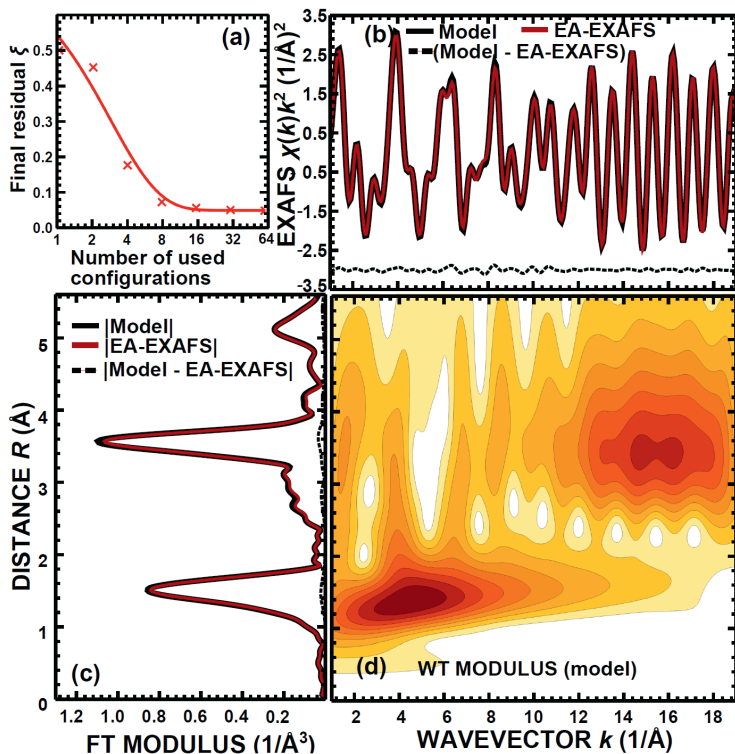


Fig. 4.1 EA analysis of ReO_3 model EXAFS spectrum

Dependence of the final residual between EA-EXAFS and MD-EXAFS on the number of simultaneously used atomic configurations in the EA method (a). The Re L_3 -edge MD-EXAFS spectrum $\chi(k)k^2$ and the one, reconstructed by the EA method using 32 atomic configurations (b), their FT moduli (c), and the WT modulus of the MD-EXAFS spectrum (d).

An increase of the number of simultaneously modelled atomic configurations, in turn, leads to almost exponential improvement. With 32 atomic configurations being used, the EA method for the same number of EXAFS calculations is able to reconstruct accurately the model data (Fig. 4.1(b) and (c)). The radial distribution functions (RDFs) around absorbing Re atom, calculated for our MD model and reconstructed by the EA method, are also in good agreement (Fig. 4.2).

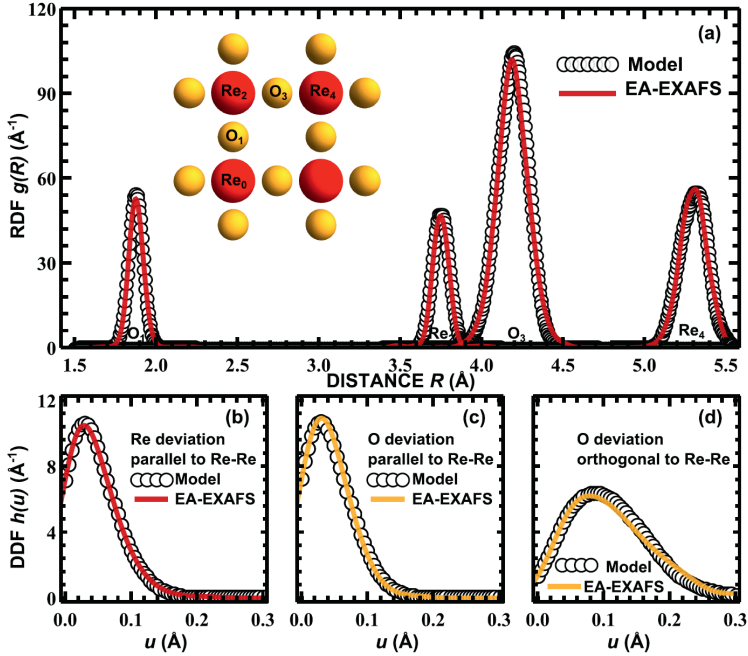


Fig. 4.2 RDF's and atomic displacements for ReO_3 model

RDF around Re atom for the first four coordination shells (Re_0 -O₁, Re_0 -Re₂, Re_0 -O₃, Re_0 -Re₄), reconstructed for the MD model by EA method and compared with RDF, obtained directly from MD coordinates (a); distributions of deviations u from equilibrium positions (DDF) for oxygen and rhenium atoms in the direction parallel and orthogonal to Re_0 -Re₂ bond, calculated using the EA method and obtained directly from MD coordinates (b-d).

4.2. Hydrogen intercalation into ReO_3 ⁵

Regarding EXAFS spectroscopy, it is necessary to note that the multiple-scattering (MS) effects are essential for crystals with cubic symmetry as rhenium trioxide (space group $Pm\bar{3}m$) [22, 23]. Due to pronounced MS effects, contributions from the second, third and further coordination shells are inaccessible for the conventional methods. On the other hand, sensitivity of EXAFS to MS effects provides the possibility to probe directly the many-atomic distribution functions, and also the correlations of different atomic displacements.

⁵ The material, presented in this section, has been published as J. Timoshenko, A. Kuzmins, J. Purans, EXAFS STUDY OF HYDROGEN INTERCALATION INTO ReO_3 USING THE EVOLUTIONARY ALGORITHM; J. Phys.: Condens. Matter 26 (2014) 055401 (15 pages).

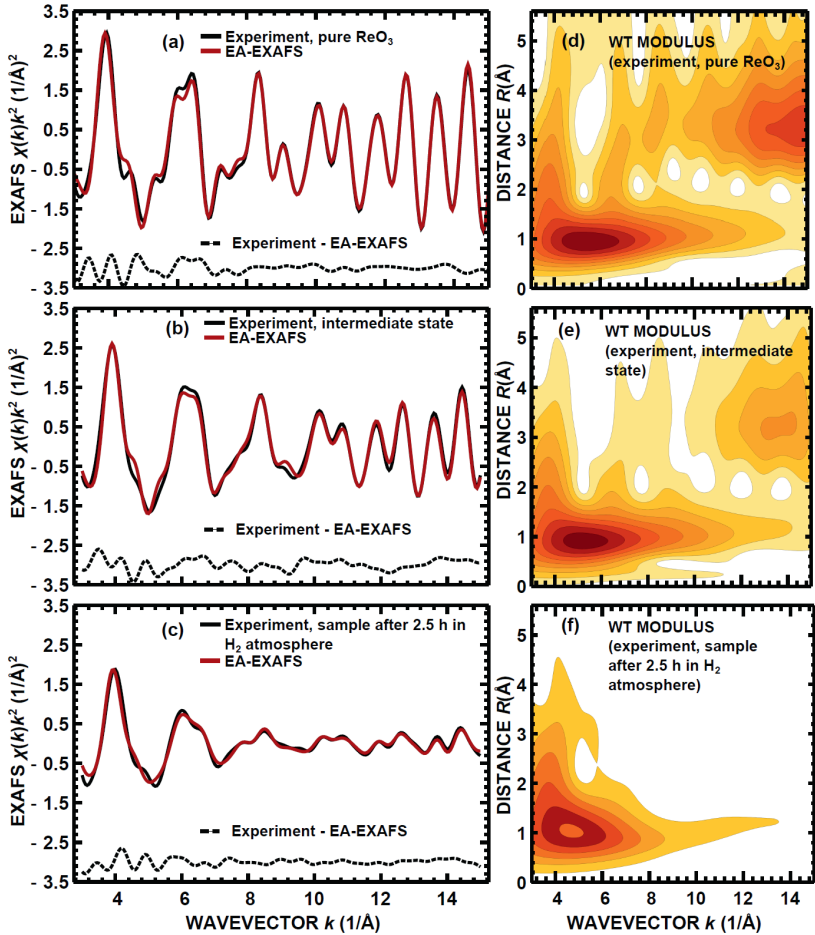


Fig. 4.3 Influence of hydrogen intercalation on EXAFS spectra

Experimental and calculated by the EA-EXAFS method Re L_{3} -edge EXAFS signals $\chi(k)k^2$ (a, b, c) and the WT moduli of experimental signals (d, e, f) for pure crystalline ReO_3 , for ReO_3 after 2.5 hours in H_2 atmosphere and for intermediate state.

In situ EXAFS measurements for the intercalation of hydrogen ions in platinized ReO_3 have been carried out in [8], where one can find also experimental details. Briefly, platinized polycrystalline ReO_3 has been exposed to hydrogen flow for 2.5 hours at room temperature. Next, the air flow was passed through the sample to oxidize it and to deintercalate the hydrogen ions. The EXAFS spectra have been *in-situ* measured before the intercalation process, after the intercalation process and continuously during the deintercalation phase. Within this thesis we carried out RMC/EA analysis of these data (Fig. 4.3).

As one can see, the significant reduction of the amplitude of EXAFS spectra, which is a result of disorder, induced by the presence of hydrogen ions, is successfully reconstructed by our RMC/EA scheme.

Thermal and static disorder in the material can be characterized by mean-square displacements (MSD) and mean-square relative displacements (MSRD) of involved atoms. MSRD factors for the first four coordination shells and the values of the MSD factors for rhenium and oxygen atoms, calculated from the atomic coordinates of the final RMC/EA models, are given in Fig. 4.4. The knowledge of both MSRD σ^2 and MSD $\langle u^2 \rangle$ quantities provides one with the access to correlation effects in atomic motion, since the two parameters are related as $\sigma^2 = \langle u^2 \rangle_A + \langle u^2 \rangle_B - \langle u_A u_B \rangle$, where $\langle u^2 \rangle_A$ and $\langle u^2 \rangle_B$ are corresponding MSD factors for atoms A and B, $\langle u_A u_B \rangle$ is the correlation of A and B atoms, and σ^2 is MSRD for A-B bond.

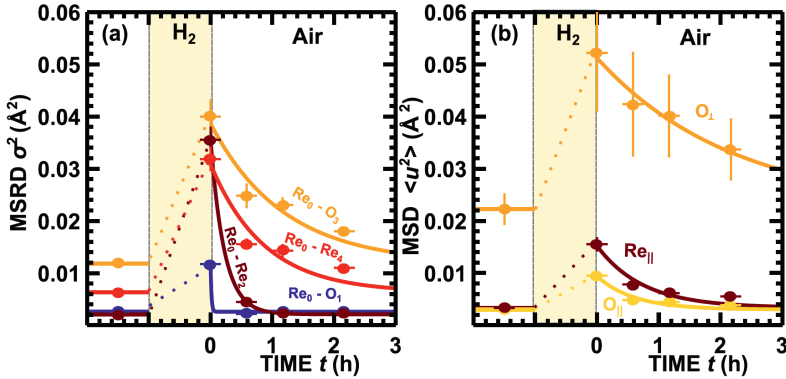


Fig. 4.4 Time-dependencies of MSRD and MSD factors in the hydrogen deintercalation process

Changes of the MSRDs for the first four coordination shells (a), and MSD factors for the displacements of Re and O atoms in the direction, parallel (..._{||}) and orthogonal (..._⊥) to the direction of Re₀-Re₂ bond, (b) in the intercalation/deintercalation process.

In pure ReO₃ the MSRD factor for the third coordination shell (O₃) is several times larger than the corresponding MSRD factors of the first (O₁) and second (Re₂) coordination shells, and also it is about twice as large as the MSRD factor of the fourth (Re₄) coordination shell. The large values of the MSRD factor for the Re₀-O₃ can be explained by (i) the large amplitude of oxygen oscillations in the direction, orthogonal to the Re₀-Re₂ bond, and (ii) relatively weak correlation of motion for Re₀ and O₃ atoms. One can estimate that the correlation effects in the Re₀-O₃ pair vibrations are negligible, since the MSRD factor for Re₀-O₃ pair (Fig. 4.4) is close to the sum of MSD factors for the two atoms $\langle u^2 \rangle_{Re} + \langle u^2 \rangle_{O_{\perp}} / 2 \approx 0.013 \text{ \AA}^2$.

As one may expect, the presence of hydrogen induces pronounced disorder in the lattice. The MSRD factor (0.036 \AA^2) for the $\text{Re}_0\text{-Re}_2$ pair increases almost 20 times in H_xReO_3 with respect to that (0.0021 \AA^2) in pure ReO_3 . It does not mean, however, that the Re lattice is completely distorted. The most significant contribution to the increase of MSRD is attributed to the reduction of the correlation in a motion of two neighbouring rhenium atoms. To estimate correlation effect, one again can compare the MSRD factor for the second coordination shell with the sum of the MSD factors for rhenium atoms, equal to $2\langle u^2 \rangle_{\text{Re}} \approx 0.0066 \text{ \AA}^2$ for pure ReO_3 and $\approx 0.031 \text{ \AA}^2$ for H_xReO_3 .

The latter value for H_xReO_3 is close to the actual value of the MSRD factor (0.036 \AA^2), whereas for pure ReO_3 it is about three times larger than the actual MSRD (0.0021 \AA^2). Thus, the motion of two neighbouring rhenium atoms is strongly correlated in pure ReO_3 , whereas it is mostly uncorrelated in H_xReO_3 .

After the sample is exposed to air, the structural parameters gradually return to the values, characteristic for pure ReO_3 . One can roughly approximate these trends with exponential functions $f(t) = f_{\text{pure}} + a \exp(-t/\tau)$ (solid lines in Fig. 4.4), where f_{pure} is the value of corresponding structural parameter (MSD or MSRD) for pure ReO_3 , a is a free parameter, t is the experimental time, and τ is the characteristic relaxation time. One can notice that the times τ differ significantly for different structure parameters. In particular, the values of τ for MSD and MSRD factors for the third (O_3) and fourth (Re_4) coordination shells, having weak correlation of atomic motion with absorbing rhenium atom, are in the range from 0.7 to 2.5 hours. On the contrary, the values of τ for MSRD factors for the first two coordination shells, which are strongly influenced by the correlation of atomic motion, are much smaller, being about 0.16 hours for the MSRD of the second (Re_2) coordination shell and even smaller (0.01 hours) for the first (O_1) coordination shell. We propose that such difference in the characteristic relaxation times is due to the fact that the changes of the structural parameters in both of these sets have different physical origin. The changes of correlation of atomic motion and, correspondingly, of MSRD factors in the first two coordination shells have electronic origin and, thus, short relaxation times. They arise due to additional electrons localized largely at rhenium atoms and introduced together with hydrogen ions to maintain charge neutrality [8].

On the contrary, the variation of the MSD and MSRD parameters in the third and fourth coordination shells reflects static disorder, caused by the presence of hydrogen atoms in the ReO_3 lattice. These variations can be associated with the tilting of ReO_6 octahedra, as observed by neutron diffraction studies [24, 25].

4.3. Anisotropic dynamics of wurtzite-type zinc oxide⁶

Zinc oxide (ZnO) is a wide band-gap semiconductor, which has many promising technological applications [26-29] and, therefore, is an extremely popular research topic during the last years [30-32]. Crystalline lattice of ZnO in most common wurtzite-type phase is essentially anisotropic [33-35] that is reflected in its piezoelectric [36] and pyroelectric [37] properties. The wurtzite structure has a hexagonal unit cell with two lattice parameters, a and c , and belongs to the space group of $P6_3mc$ [26].

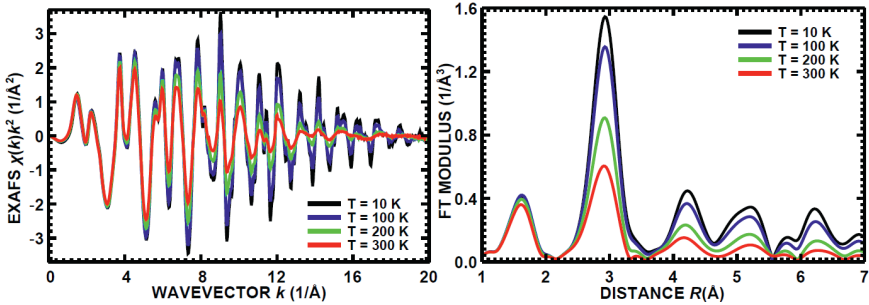


Fig. 4.5 Experimental Zn K-edge EXAFS spectra for zinc oxide

Experimental spectra $\chi(k)k^2$ and they Fourier transforms (FT) for polycrystalline wurtzite-type ZnO, measured at temperatures from 10 K to 300 K.

Lattice is composed of two interpenetrating hexagonal-close-packed sublattices, each built up by one type of atoms (Zn or O), which are displaced with respect to each other along the threefold c -axis by the amount of the internal parameter u . Both Zn and O atoms are tetrahedrally coordinated by four atoms of the other type, and the value of the parameter u controls the degree of the ZnO_4 tetrahedra distortion.

In this study we employed reverse Monte Carlo method coupled with evolutionary algorithm for the analysis of temperature-dependent (10-300 K) Zn K-edge EXAFS data from polycrystalline wurtzite-type ZnO, taking into account all important MS contributions, anisotropy of the system and also the thermal disorder effects.

⁶ The material, presented in this section, has been published as J. Timoshenko, A. Anspoks, A. Kalinko, A. Kuzmin, LOCAL STRUCTURE AND DYNAMICS OF WURTZITE-TYPE ZnO FROM SIMULATION-BASED EXAFS ANALYSIS, Phys. Stat. Solidi (c) 11 (2014) 1472- 1475; and as J. Timoshenko, A. Anspoks, A. Kalinko, A. Kuzmin, TEMPERATURE DEPENDENCE OF THE LOCAL STRUCTURE AND LATTICE DYNAMICS OF WURTZITE-TYPE ZnO, Acta Mater. 79 (2014) 194-202.

X-ray absorption spectra of wurtzite-type ZnO (99.99%, Alfa Aesar) were acquired at the HASYLAB/DESY C bending-magnet beamline [38]. A liquid He flow cryostat was used to control sample temperature.

The supercell, used in the calculations, the experimental ($T = 300$ K) EXAFS spectrum and the calculated EXAFS spectrum corresponding to the final RMC/EA configuration (RMC/EA-EXAFS) are shown in Fig. 4.6, along with the corresponding Fourier and wavelet images. A good agreement between the experimental and calculated Zn K-edge EXAFS spectra is achieved both in k and R space. This result suggests that the structural model, obtained by the RMC/EA method, is reliable enough to be used in further analysis for the extraction of more detailed information.

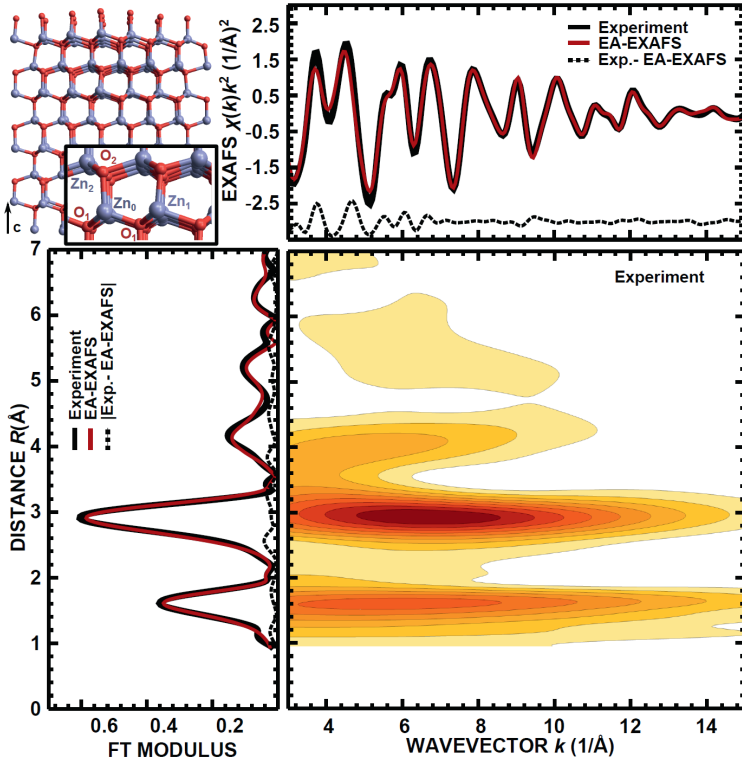


Fig. 4.6 RMC/EA simulations for 300 K temperature experimental EXAFS data

Upper left panel: supercell used in the RMC/EA simulation (blue large balls are zinc atoms, red small balls are oxygen atoms). Upper right panel: the experimental ($T = 300$ K) and calculated K-edge EXAFS spectra and their difference. Bottom left panel: Fourier transforms of the experimental and calculated EXAFS spectra and their difference. Bottom right panel: the wavelet transform of the experimental EXAFS spectrum.

According to the X-ray diffraction data [34, 35] (see dashed lines in Fig. 4.7), the average distances $\langle R \rangle_D(\text{Zn}_0\text{-Zn}_1)$ and $\langle R \rangle_D(\text{Zn}_0\text{-Zn}_2)$ should vary little solely due to the lattice thermal expansion. However, the interatomic distances, as revealed by our RMC/EA-EXAFS analysis, (circles in Fig. 4.7) grow with increasing temperature due to the additional contribution caused by thermal vibrations [39].

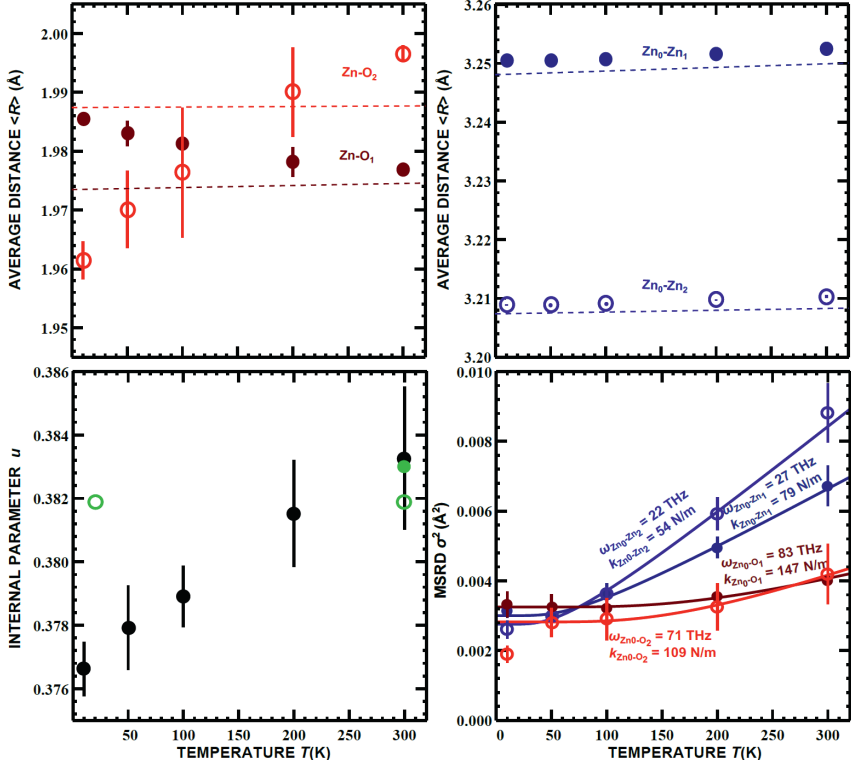


Fig. 4.7 Structure parameters for wurtzite-type ZnO

Upper panels: temperature dependences of Zn-O (left panel) and Zn-Zn (right panel) average interatomic distances; dashed lines show X-ray diffraction data in the range from 4.2 to 300 K from [34, 35]. Lower left panel: temperature dependence of the internal parameter u , obtained from our RMC/EA simulations; the values of the parameter u obtained from diffraction studies are shown by green empty circles (neutron diffraction [42]) and green filled circle (X-ray diffraction [43]). Lower right panel: MSD factors as a function of temperature for the four atom pairs (Zn₀-O₁, Zn₀-O₂, Zn₀-Zn₁ and Zn₀-Zn₂); solid lines: fits by the Einstein model).

At the same time, the average distances between zinc and four nearest oxygen atoms, forming ZnO₄ tetrahedron, vary differently with increasing

temperature. The average distance $\langle R \rangle_{EXAFS}(Zn_0-O_2)$ between the absorbing zinc and the apical oxygen atom, located along the c -axis, increases, whereas the average distance $\langle R \rangle_{EXAFS}(Zn_0-O_1)$ between the absorbing zinc and the three basal oxygen atoms, located within the ab -plane, is slightly reduced. This result is a consequence of variations of the internal parameter u . Our analysis shows that the parameter u increases by about 0.01 with increasing temperature from 10 K to 300 K. This result is especially intriguing, since it is known that the parameter u is responsible for pyroelectric properties of wurtzite-type compounds [40].

Temperature dependencies of the parallel MSRD's for the four atom pairs (Zn_0-O_1 , Zn_0-O_2 , Zn_0-Zn_1 and Zn_0-Zn_2) were fitted using correlated Einstein model [41] (bottom right panel of Fig. 4.7). The obtained values of the Einstein frequency ω were used to estimate effective bond-strength constants κ .

The obtained results suggest that the atoms, located within one ab -plane (i.e., Zn_0-Zn_1 and Zn_0-O_1 atom pairs) are interacting more strongly than the atoms, located in the neighbouring layers along the c -axis (Zn_0-Zn_2 and Zn_0-O_2 atom pairs), although the distances between, correspondingly, Zn_0-Zn_1 and Zn_0-Zn_2 , and Zn_0-O_1 and Zn_0-O_2 are close.

4.4. Structure of nanosized tungstates⁷

$CoWO_4$ and $CuWO_4$ are wolframite-type compounds [44]. Cobalt tungstate has monoclinic structure (space group $P2/c$) [45, 46], while $CuWO_4$ has even lower, triclinic symmetry (space group $P\bar{1}$) [45-47]. The low symmetry of these compounds is due to (i) the first-order Jahn-Teller effect that results in deformation of CuO_6 octahedra in $CuWO_4$, and (ii) the second-order Jahn-Teller effect that deforms the WO_6 octahedra in both $CoWO_4$ and $CuWO_4$.

Both $CoWO_4$ and $CuWO_4$ are promising catalytic materials, for instance, for photocatalytic oxidation of water. Catalytic properties of these compounds are especially pronounced in their nanostructured form. Thus the properties of such materials strongly depend on the atomic structure, which, in turn, for nanostructured sample can significantly differ from that in the bulk.

X-ray absorption spectroscopy may be a proper tool to investigate the structure of wolframite-type compounds due to its local sensitivity and element selectivity [3]. In this work to reconstruct the 3D structure of nanocrystalline

⁷ The material, presented in this section, has been published as J. Timoshenko, A. Anspoks, A. Kalinko, A. Kuzmin, ANALYSIS OF EXAFS DATA FROM COPPER TUNGSTATE BY REVERSE MONTE CARLO METHOD, *Physica Scripta* 89 (2014) 044006 (6 pages); and as J. Timoshenko, A. Anspoks, A. Kalinko, A. Kuzmin, LOCAL STRUCTURE OF NANO-SIZED TUNGSTATES REVEALED BY EVOLUTIONARY ALGORITHM (accepted for publication in *Physica Status Solidi A* in 2014).

CuWO₄ and CoWO₄ we analyze corresponding EXAFS data using the reverse Monte Carlo and evolutionary algorithm technique.

X-ray absorption measurements were performed in transmission mode at the HASYLAB/DESY C1 bending-magnet beamline at the Co and Cu K and W L₃-edges. Nanocrystalline CoWO₄ and CuWO₄ powder samples were obtained by co-precipitation method from aqueous solutions [48, 49]. Microcrystalline powders were obtained from nanopowders by annealing at 800°C for 4-8 hours. Both microcrystalline and nanocrystalline samples were previously characterized using Raman spectroscopy, FTIR measurements and X-ray diffraction: nanosized tungstates appeared to be X-ray amorphous, which indicates that the synthesized nanocrystallites are just a few nanometers large.

Room temperature EXAFS data for microcrystalline and nanocrystalline CoWO₄ and their Fourier transforms are compared in Fig. 4.8. One can note that the amplitude of EXAFS for nanocrystalline CoWO₄ is significantly smaller (especially for W L₃-edge spectrum) suggesting strong structure distortion due to size reduction and accompanying structure relaxation effects.

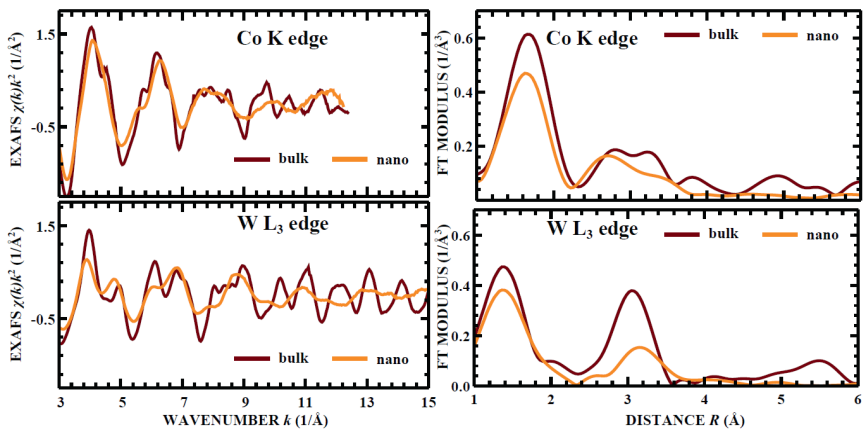


Fig. 4.8 EXAFS spectra for nanocrystalline CoWO₄

Experimental Co K-edge and W L₃-edge room temperature EXAFS spectra for microcrystalline (“bulk”) and nanocrystalline (“nano”) CoWO₄ and their Fourier transforms.

The FT peaks beyond the second one are almost completely suppressed for nanocrystalline CoWO₄, indicating the lack of order beyond the first few coordination shells. This may be interpreted as an evidence of the very small size of nanoparticles.

In this section for the first time our RMC/EA-EXAFS approach is applied to reconstruct the structure of nanomaterials. Since the experimentally

measured CoWO_4 and CuWO_4 EXAFS spectra are averaged over large number of nanoparticles, as a starting configuration an ensemble of 64 identical nanoparticles was used. These nanoparticles consist of four WO_6 and CoO_6 (or CuO_6) octahedra and correspond to one of the four proposed models (A, B, C, D, see Fig. 4.9).

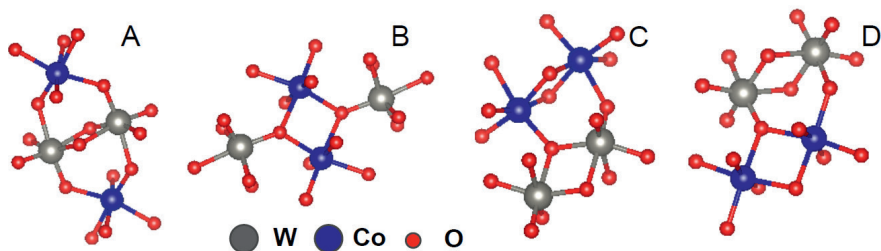


Fig. 4.9 Suggested structure models of CoWO_4 nanocrystallites

Additional complication arises from the fact, observed in the studies for polycrystalline CoWO_4 and CuWO_4 , that EXAFS spectrum, measured at single absorption edge, does not contain sufficient information to unambiguously reconstruct the 3D structure of such complex materials. The influence of multiple-scattering effects is small in the observed systems, therefore EXAFS is determined practically only by pair-distribution functions of involved atoms and contains, for instance, no information on bonding angles.

To treat the above mentioned problem, we perform RMC/EA fit of the Co (Cu) K-edge and W L_3 -edge EXAFS spectra simultaneously, using a single structural model for both spectra.

The experimental Co K-edge and W L_3 -edge EXAFS spectra from nanocrystalline CoWO_4 at room temperature and their Fourier transforms along with the results of EA simulations starting from four different structural models are shown in Fig. 4.10. Similar results were obtained also for nanocrystalline CuWO_4 at room temperature and at 10 K.

As one can see, all four models (A, B, C and D) are able to reproduce the experimental EXAFS spectra from the first coordination shell (broad, asymmetric peaks in FTs between 1 and 2 Å) around metal atoms, thus confirming that the building elements of nanosized tungstates are distorted metal-oxygen octahedra.

The main differences between the results, obtained for the four proposed models, are observed in the further peaks of FTs that are located between 2 and 4 Å and correspond to the contribution from the further coordination shells and multiple-scattering effects – i.e., to the part of EXAFS that is difficult to access precisely by conventional methods.

In the FTs in Fig. 4.10 it is seen that the model A (i.e., the model without edge-sharing CuO_6 (CoO_6) octahedra) contradicts the obtained experimental Co K-edge EXAFS data: the amplitude of FT peaks for simulated spectra is much lower than that for the experimental spectra.

Models B, C and D with edge-sharing CoO_6 octahedra give similar and quite remarkable results: the agreement between calculated EXAFS spectra and experimental Co K-edge and W L_3 -edge data is excellent even for the complex peaks at 2-4 Å. Careful examination of the final total differences between calculated and experimental EXAFS at both Co(Cu) K and W L_3 edges shows that the model B (i.e., the model without edge-sharing WO_6 octahedra) describes slightly better the obtained experimental data for both CoWO_4 and CuWO_4 cases: this model provides slightly better agreement for the W L_3 -edge EXAFS. Note that the presence of two neighboring Co or Cu atoms as in models B, C and D is required for Langmuir-Hinshelwood-like mechanism of water oxidation reaction [50], thus our result is consistent with the observed high catalytic activity of tungstate nanoparticles.

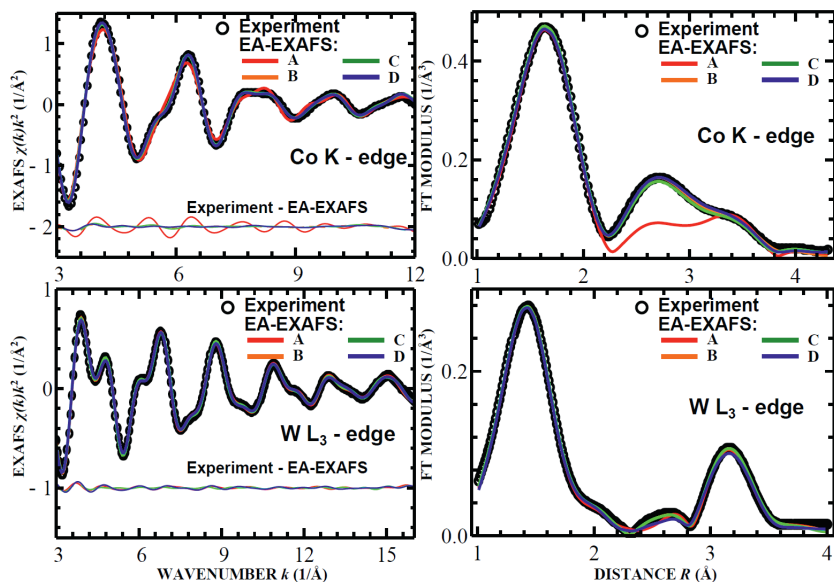


Fig. 4.10 RMC/EA analysis of EXAFS spectra for nanocrystalline CoWO_4

Left panels: the experimental Co K-edge and W L_3 -edge EXAFS spectra for nanocrystalline CoWO_4 at room temperature are shown by circles and the results of RMC/EA simulations starting from four different structural models (A, B, C, D as in Fig. 4.9) are represented by thick solid lines. Thin solid lines in the left panels show the difference between experimental EXAFS and the result of corresponding RMC/EA calculation. Right panels: the corresponding Fourier transforms are shown.

5. CONCLUSIONS

In this thesis we have presented a novel reverse Monte Carlo (RMC) – type approach for the advanced analysis of EXAFS data for crystalline and nano-crystalline materials. A number of original features in our approach allows us to outperform other existing methods in this field in the terms of computational efficiency and the complexity of information that can be obtained. Let us emphasize them here once again.

First of all, we considered that the complex structure of EXAFS spectra due to a contribution of the multiple-scattering effects and of distant coordination shells is not an obstacle, but rather a source of valuable structural information that can be treated using simulation-based approaches and possibilities, provided by modern *ab-initio* codes for EXAFS data modelling. While such advanced analysis is computationally expensive, it allows one to discover a new potentiality of the EXAFS spectroscopy as a method not only for local structure studies, but also for probing more distant coordination shells, for revealing the anisotropy and correlations of atomic thermal motion and static displacements, for investigations of bonding angles and more complex many-atom distribution functions. These possibilities can bring new light even to studies of relatively well-known materials as was demonstrated in this thesis, for instance, on the example of the analysis of EXAFS data for wurtzite-type ZnO, where RMC-type approach allowed us to reveal essential differences between dynamics of Zn-O and Zn-Zn bonds aligned along the *c*-axis and in the *ab*-plane of ZnO hexagonal crystal lattice.

Secondly, as it was shown, the optimization process that employs the power of evolutionary algorithm (EA), implemented by us for the first time for simulation-based EXAFS analysis, allows much more efficient exploration of the possible configuration space (in our case – configurations of atomic coordinates in 3D structure model). This approach allowed us to make feasible advanced analysis of complex compounds with low symmetry even with only decent computational resources available. We would like to emphasize that this aspect is very important to make the approach, presented here, broadly available and applicable to many other material studies. Computational efficiency of the method is also an issue, when one considers that to extract the dynamical information from EXAFS measurements it is not enough to interpret a single spectrum. Instead one should analyze a whole series of experimental data, obtained, for instance, at different temperatures. This approach revealed the displacement of equilibrium position of oxygen atoms along *c*-axis of hexagonal ZnO lattice. Obviously, the same principle applies to the processing of EXAFS from any *in-situ* experiment, and within this thesis we presented the results of RMC/EA study of EXAFS data for the *in-situ* measurements of hydrogen intercalation/deintercalation process into ReO₃ lattice. We were able to reveal

and distinguish two different effects that are caused by insertion of H^+ ions: the changes in the correlation of atomic motion due to the localization of additional electron and the distortion of rhenium-oxygen octahedra.

Thirdly, the wavelet analysis has been applied for the first time for quantitative EXAFS interpretation. The representation of EXAFS spectra in real and frequency spaces simultaneously using wavelet transform (WT) allowed us to obtain more information from the same experimental data and to have much better control over the difference between the experimental and calculated EXAFS data. Especially useful the WT turns to be for the analysis of EXAFS data from the materials, containing both light and heavy elements, such as transition-metal oxides (e.g., ReO_3 and ZnO), tungstates (e.g., $CuWO_4$ and $CoWO_4$), etc. Note that the usage of WT can be advantageous even for conventional EXAFS analysis (curve-fitting).

As it is with a solution to any inverse ill-posed problem, the information, obtained by RMC-type methods, should be taken cautiously and cross-checked with other available experimental and theoretical data. In our approach we have constrained the allowed atomic displacements from the known equilibrium positions to be smaller than some given value. It allowed us to stabilize the solution and to incorporate indirectly the results of diffraction experiments. This aspect, however, limits the presented approach to the analysis of crystalline materials. Within this thesis it was also demonstrated that for the analysis of complex materials, such as cobalt and copper tungstates, the use of EXAFS data at several absorption edges (e.g., $W L_3$ -edge and $Co/Cu K$ -edge) is required to obtain unambiguous solution. Luckily, the RMC/EA-type approach allows simultaneous analysis of several EXAFS spectra in a straightforward way. Important step in the development of our method was also the validation of its stability and precision of different obtainable structural parameters, by applying it to the analysis of model EXAFS data, based on molecular dynamics (MD) simulations. Thus MD calculations can be used to check the results of RMC analysis. On the other hand, the RMC/EA-EXAFS approach allows us to identify the problems with the force fields, used for molecular dynamics calculations.

One can expect that in the future different combinations of our RMC/EA and other numerical simulations can provide even more insight on the local structure and dynamics of different materials. Especially intriguing is the possibility to use the results, provided by our RMC implementation, i.e., the 3D structural model, consistent with available experimental data, for *ab-initio* calculations of electronic structure, and, hence, chemical and optical properties of materials.

Finally, in this thesis it was shown that the developed RMC/EA approach allows us also to validate the consistency of different structure models with available experimental data: in particular, we have shown that the nanoparticles

of CoWO_4 and CuWO_4 consist of WO_6 and CoO_6 (CuO_6) octahedra. Moreover, our analysis of EXAFS data beyond the first coordination shell that was made possible by presented RMC/EA scheme, has shown that CoO_6 (CuO_6) octahedra have common edges, while the WO_6 octahedra probably do not. This example introduces a very promising and broad field of future studies, where the approach, presented in this thesis, is applied to investigation of not only crystalline solids, but also of materials, where the equilibrium structure is not known *a-priori*: i.e., various nanostructured materials, complex mixtures, solid solutions and disordered solids.

6. MAIN THESES

The main results of this thesis are:

1. The developed reverse Monte Carlo/evolutionary algorithm method allows one to efficiently analyze EXAFS data for crystalline and nanocrystalline materials, taking into account static and thermal disorder and multiple-scattering effects.
2. The intercalation of hydrogen ions into ReO_3 lattice leads to two different effects with different characteristic times: (i) the reduction of correlations in atomic motion that occurs relatively fast and (ii) the tilting of ReO_6 octahedra that is much slower process. The significant reduction of the Re L_3 -edge EXAFS amplitude from H_xReO_3 compound in comparison with that from pure ReO_3 mostly is a result of changes of atomic correlations.
3. The analysis of the Zn K-edge EXAFS spectra suggests that the lattice dynamics of ZnO is essentially anisotropic: the interactions of atoms that lies in the same ab -plane are significantly different from the interactions of atoms that are located at similar distances but in different ab -planes. As a result, the equilibrium position of oxygen atoms along c -axis changes upon increasing temperature.
4. Simultaneous analysis of EXAFS spectra at the Co/Cu K-edge and W L_3 -edge in CoWO_4 and CuWO_4 nanoparticles allows one to reconstruct their atomic structure. It is shown that the nanoparticles consist of a few distorted WO_6 and $\text{Co}(\text{Cu})\text{O}_6$ octahedra, where the latter ones are connected by edges.

REFERENCES

- [1] S. J. Billinge and I. Levin. *Science* 316 (2007) 561.
- [2] A. Filippini. *J. Phys.: Condens. Matter* 13 (2001) R23.
- [3] J. J. Rehr and R. C. Albers. *Rev. Mod. Phys.* 72 (2000) 621.
- [4] A. Kuzmin and R. Evarestov. *J. Phys.: Condens. Matter* 21 (2009) 055401.
- [5] D. F. Yancey, S. T. Chill, L. Zhang et al. *Chem. Sci.* 4 (2013) 2912.
- [6] S. J. Gurman and R. L. McGreevy. *J. Phys.: Condens. Matter* 2 (1990) 9463.
- [7] J. Purans, N. D. Afify, G. Dalba et al. *Phys. Rev. Lett.* 100 (2008) 055901.
- [8] J. Gaidelene, A. Kuzmin, J. Purans et al. *Phys. Status Solidi C* 2 (2005) 149.
- [9] A. Kuzmin. *Latvian J. Phys. Tech. Sci.* 2 (2006) 7.
- [10] A. L. Ankudinov, B. Ravel, J. J. Rehr et al. *Phys. Rev. B* 58 (1998) 7565.
- [11] A. Filippini, A. D. Cicco and C. R. Natoli. *Phys. Rev. B* 52 (1995) 15122.
- [12] N. Metropolis, A. W. Rosenbluth, M. N. Rosenbluth et al. *J. Chem. Phys.* 21 (1953) 1087.
- [13] R. McGreevy and L. Pusztai. *Mol. Simul.* 1 (1988) 359.
- [14] M. G. Tucker, D. A. Keen, M. T. Dove et al. *J. Phys.: Condens. Matter* 19 (2007) 335218.
- [15] I.-K. Jeong and J. Ahn. *Appl. Phys. Lett.* 101 (2012) 242901.
- [16] A. D. Cicco, A. Trapananti, S. Faggioni et al. *Phys. Rev. Lett.* 91 (2003) 135505.
- [17] P. Jóvári, P. Lucas, Z. Yang et al. *J. Am. Ceram. Soc.* 97 (2014) 1625.
- [18] V. Krayzman, I. Levin, J. C. Woicik et al. *J. Appl. Cryst.* 42 (2009) 867.
- [19] M. Munóz, P. Argoul and F. Farges. *Am. Mineral.* 88 (2003) 694.
- [20] J. Holland. *Adaptation in natural and artificial systems: an introductory analysis with applications to biology, control, and artificial intelligence*. MIT Press (1992). ISBN 978-0262581110.
- [21] A. Kalinko, R. A. Evarestov, A. Kuzmin et al. *J. Phys.: Conf. Ser.* 190 (2009) 012080.
- [22] N. Alberding, E. Crozier, R. Ingalls et al. *Le Journal de Physique Colloques* 47 (1986) C8.
- [23] A. Kuzmin, J. Purans, M. Benfatto et al. *Phys. Rev. B* 47 (1993) 2480.
- [24] P. Dickens and M. Weller. *J. Solid State Chem.* 48 (1983) 407.
- [25] G. D. Barrera, J. A. O. Bruno, T. H. K. Barron et al. *J. Phys.: Condens. Matter* 17 (2005) R217.
- [26] U. Özgür, Y. I. Alivov, C. Liu et al. *J. Appl. Phys.* 98 (2005) 041301.
- [27] M. Willander, O. Nur, Q. X. Zhao et al. *Nanotech.* 20 (2009) 332001.
- [28] A. I. Hochbaum and P. Yang. *Chem. Rev.* 110 (2010) 527.
- [29] P. D. C. King and T. D. Veal. *J. Phys.: Condens. Matter* 23 (2011) 334214.
- [30] S. Pearton, D. Norton, K. Ip et al. *Prog. Mat. Sci.* 50 (2005) 293.
- [31] S. Singh, P. Thiagarajan, K. Mohan Kant et al. *J. Phys. D: Appl. Phys.* 40 (2007) 6312.
- [32] A. Janotti and C. G. Van de Walle. *Rep. Prog. Phys.* 72 (2009) 126501.
- [33] S. C. Abrahams and J. L. Bernstein. *Acta Crystall. B* 25 (1969) 1233.
- [34] R. R. Reeber. *J. Appl. Phys.* 41 (1970) 5063.
- [35] H. Karzel, W. Potzel, M. Köfferlein et al. *Phys. Rev. B* 53 (1996) 11425.
- [36] Z. L. Wang and J. Song. *Science* 312 (2006) 242.
- [37] Y. Yang, W. Guo, K. C. Pradel et al. *Nano Lett.* 12 (2012) 2833.

- [38] K. Rickers, W. Drube, H. Schulte-Schrepping et al. AIP Conf. Proc. 882 (2007) 905.
- [39] P. Fornasini. J. Phys.: Condens. Matter 13 (2001) 7859.
- [40] S. L. Mair and Z. Barnea. Acta Crystallogr. A 31 (1975) 201.
- [41] E. Sevillano, H. Meuth and J. J. Rehr. Phys. Rev. B 20 (1979) 4908.
- [42] J. Albertsson, S. Abrahams and Å. Kvik. Acta Crystallogr. B 45 (1989) 34.
- [43] K. Kihara and G. Donnay. Can. Mineral. 23 (1985) 647.
- [44] H. Weitzel. Solid State Commun. 8 (1970) 2071.
- [45] S. Naik and A. Salker. Solid State Sci. 12 (2010) 2065.
- [46] J. B. Forsyth, C. Wilkinson and A. I. Zvyagin. J. Phys.: Condens. Matter 3 (1991) 8433.
- [47] A. Anders, A. Zvyagin, M. Kobets et al. Sov. Phys. JETP 35 (1972).
- [48] A. Kalinko and A. Kuzmin. J. Lumin. 129 (2009) 1144.
- [49] A. Kalinko and A. Kuzmin. J. Non-Cryst. Solids 357 (2011) 2595.
- [50] H. Jia, J. Stark, L. Q. Zhou et al. RSC Advances 2 (2012) 10874.

AUTHOR'S PUBLICATION LIST

Published papers

1. J. Timoshenko, A. Kuzmin, WAVELET DATA ANALYSIS OF EXAFS SPECTRA, *Comp. Phys. Commun.* 180 (2009) 920-925.
2. J. Purans, J. Timoshenko, A. Kuzmin, G. Dalba, P. Fornasini, R. Grisenti, N. D. Afify, F. Rocca, S. De Panfilis, I. Ozhogin, and S. I. Tiutiunnikov, FEMTOMETER ACCURACY EXAFS MEASUREMENTS: ISOTOPIC EFFECT IN THE FIRST, SECOND AND THIRD COORDINATION SHELLS OF GERMANIUM, *J. Phys.: Conf. Ser.* 190 (2009) 012063 (6 pages).
3. A. Anspoks, A. Kuzmin, A. Kalinko, J. Timoshenko, PROBING NiO NANOCRYSTALS BY EXAFS SPECTROSCOPY, *Solid State Commun.* 150 (2010) 2270-2274.
4. J. Timoshenko, A. Kuzmin, J. Purans, MOLECULAR DYNAMICS SIMULATIONS OF EXAFS IN GERMANIUM, *Cent. Eur. J. Phys.* 9 (2011) 710-715.
5. J. Timoshenko, A. Kuzmin, J. Purans, REVERSE MONTE CARLO MODELLING OF THERMAL DISORDER IN CRYSTALLINE MATERIALS FROM EXAFS SPECTRA, *Comp. Phys. Commun.* 183 (2012) 1237-1245.
6. J. Timoshenko, A. Kuzmin, J. Purans, AN EFFICIENT IMPLEMENTATION OF THE REVERSE MONTE CARLO METHOD FOR EXAFS ANALYSIS IN CRYSTALLINE MATERIALS, *J. Phys.: Conf. Ser.* 430 (2013) 012012 (4 pages).
7. A. Kuzmin, A. Anspoks, A. Kalinko, J. Timoshenko, EFFECT OF COBALT DOPING ON THE LOCAL STRUCTURE AND DYNAMICS OF MULTIFERROIC MnWO_4 and $\text{Mn}_{0.7}\text{Co}_{0.3}\text{WO}_4$ *J. Phys.: Conf. Ser.* 430 (2013) 012109 (4 pages).
8. J. Timoshenko, A. Anspoks, A. Kalinko, A. Kuzmin, ANALYSIS OF EXAFS DATA FROM COPPER TUNGSTATE BY REVERSE MONTE CARLO METHOD, *Phys. Scripta* 89 (2014) 044006 (6 pages).
9. J. Timoshenko, A. Kuzmin, J. Purans, EXAFS STUDY OF HYDROGEN INTERCALATION INTO ReO_3 USING THE EVOLUTIONARY ALGORITHM, *J. Phys.: Condens. Mat.* 26 (2014) 055401 (15 pages). **IOF Editor Selected Article.**
10. A. Anspoks, A. Kalinko, J. Timoshenko, A. Kuzmin, LOCAL STRUCTURE RELAXATION IN NANOSIZED TUNGSTATES, *Solid State Commun.* 183 (2014) 22-26.
11. A. Kuzmin, A. Anspoks, A. Kalinko, J. Timoshenko, R. Kalendarev, X-RAY ABSORPTION SPECTROSCOPY OF Cu-DOPED WO_3 FILMS FOR USE IN ELECTROCHEMICAL METALLIZATION CELL MEMORY, *J. Non-Cryst. Solids* 401 (2014) 87-91. (5 pages).
12. A. Kuzmin, A. Anspoks, A. Kalinko, J. Timoshenko, R. Kalendarev, EXAFS SPECTROSCOPY AND FIRST-PRINCIPLES STUDY OF SnWO_4 , *Phys. Scripta* 89 (2014) 044005 (5 pages).
13. J. Timoshenko, A. Anspoks, A. Kalinko, A. Kuzmin, TEMPERATURE DEPENDENCE OF THE LOCAL STRUCTURE AND LATTICE DYNAMICS OF WURTZITE-TYPE ZnO , *Acta Mater.* 79 (2014) 194-202.
14. J. Timoshenko, A. Anspoks, A. Kalinko, A. Kuzmin, LOCAL STRUCTURE AND DYNAMICS OF WURTZITE-TYPE ZnO FROM SIMULATION-BASED EXAFS ANALYSIS, *Phys. Status Solidi C* 11 (2014) 1472-1475.

15. J. Timoshenko, A. Anspoks, A. Kalinko and A. Kuzmin, LOCAL STRUCTURE OF NANOSIZED TUNGSTATES REVEALED BY EVOLUTIONARY ALGORITHM; accepted for publication in *Physica Status Solidi A* in 2014.

Papers, submitted for publication

1. J. Timoshenko, A. Anspoks, A. Kalinko and A. Kuzmin, ANALYSIS OF EXAFS DATA FROM COBALT TUNGSTATE CoWO_4 : REVERSE MONTE CARLO APPROACH; submitted for publication in *Journal of Physics: Conference Series*.
2. J. Timoshenko, A. Anspoks, A. Kalinko, I. Jonane, A. Kuzmin, LOCAL STRUCTURE OF MULTIFERROIC $\text{Mn}_{1-c}\text{Co}_c\text{WO}_4$ SOLID SOLUTIONS REVEALED BY THE EVOLUTIONARY ALGORITHM; submitted for publication in *Ferroelectrics*.

Published papers that are not related to the topic of the thesis

1. V. Kashcheyevs, J. Timoshenko, QUANTUM FLUCTUATIONS AND COHERENCE IN HIGH-PRECISION SINGLE-ELECTRON CAPTURE, *Phys. Rev. Lett.* 109 (2012) 216801 (5 pages).
2. L. Fricke, M. Wulf, B. Kaestner, V. Kashcheyevs, J. Timoshenko, P. Nazarov, F. Hohls, P. Mirovsky, B. Mackrodt, R. Dolata, T. Weimann, K. Pierz, H. W. Schumacher, COUNTING STATISTICS FOR ELECTRON CAPTURE IN A DYNAMIC QUANTUM DOT, *Phys. Rev. Lett.* 110 (2013) 126803 (5 pages). **PRL Editor Suggested Article.**